Phototroph-heterotroph interactions during growth and long-term starvation across *Prochlorococcus* and *Alteromonas* diversity

Osnat Weissberg*, Dikla Aharonovich* and Daniel Sher

Department of Marine Biology, Leon H. Charney School of Marine Sciences, University of Haifa, Israel

* Dikla Aharonovich and Osnat Weissberg contributed equally to this study

Correspondence: dsher@univ.haifa.ac.il

Running title: *Prochlorococcus-Alteromonas* interactions across diversity

Abstract

Interactions among microorganisms are ubiquitous, yet to what extent strain-level diversity affects interactions is unclear. Phototroph-heterotroph interactions in marine environments have been studied intensively, due to their potential impact on ocean ecosystems and biogeochemistry. Here, we characterize the interactions between five strains each of two globally abundant marine bacteria, *Prochlorococcus* (a phototroph) and *Alteromonas* (a heterotroph), from the first encounter between individual strains and over more than a year of subsequent co-culturing. *Prochlorococcus-Alteromonas* interactions affected primarily the dynamics of culture decline, which we interpret as representing cell mortality and lysis. The shape of the decline curve and the carrying capacity of the co-cultures were determined by the phototroph and not the heterotroph strains involved. Comparing various models of culture mortality suggests that death rate increases over time in mono-cultures but decreases in co-cultures, with cells potentially becoming more resistant to stress. During 435 days of co-culture, mutations accumulated in one *Prochlorococcus* strain (MIT9313) in genes involved in nitrogen metabolism and the stringent response, indicating that these processes occur during long-term nitrogen starvation. Our results suggest potential mechanisms involved in long-term starvation survival in co-culture, and highlight the information-rich growth and death curves as a useful readout of the interaction phenotype.

Keywords: Microbial interactions, growth curves, machine learning, mortality, co-culture

Introduction

Interactions among microorganisms occur in every known ecosystem. Positive (synergistic) interactions allow organisms to exchange resources, potentially increasing biodiversity, whereas negative interactions such as competition, allelopathy and predation may lead to organisms displacing one another (recently reviewed by (Fritts et al., 2021; Gralka et al., 2020)). Detailed studies of the interactions between selected model organisms (often in laboratory co-cultures) have begun to reveal the diversity of molecular mechanisms whereby organisms interact with each other (Fritts et al., 2021; Harrington et al., 2021; Weisskopf et al., 2021). However, it is currently unknown to what extent the studied interactions are conserved across organisms, growth stages or environmental conditions. For example, while broad-scale phylogenetic patterns are often observed in microbial interactions, closely related bacteria may differ in the way they interact with other organisms, likely as a result of the significant genetic diversity observed in many microbial clades (e.g. (Cordero et al., 2012; Long & Azam, 2001)). Additionally, the same pair of interacting organisms can synergize or compete depending on the composition of the culture media and the growth stage of (co)-culture (e.g. (Grossart & Simon, 2007; Segev et al., 2016; Seyedsayamdost et al., 2011). Finally, both the coarse-grained ecological classification of microbial interactions (e.g. positive/negative) and the high-resolution mechanistic view obtained using advanced physiology and omics approaches are difficult to translate into quantitative, predictive models of organismal growth and decline (Antoniewicz, 2020; Gralka et al., 2020; Zoccarato et al., 2020) . Therefore, we still face fundamental challenges in interpreting and understanding the increasingly diverse and mechanistic view of microbial interactions and translating these insights into conceptual and mathematical models of cell growth and death.

Growth curves from batch (co)-cultures are information-rich views of microbial growth and mortality, which can provide an important link between the phenotypic outcome of microbial interactions and the underlying mechanism. Growth curves can be divided into discrete phases (lag, exponential, stationary, decline and long-term stationary phases), and can be used to extract quantitative parameters such as growth rates, lag times, etc. (Sher et al., 2011; Warringer et al., 2008). An extra layer of more subtle information may exist in the shapes of the growth curves, providing hints of important shifts in the physiology of the growing organisms, as classically demonstrated for diauxic growth in *E. coli* (Monod, 1949). Notably, while many studies of bacterial interactions focus on the exponential growth stage or on culture yield at a specific time-point (e.g. (Foster & Bell, 2012; Pacheco et al., 2021; Vetsigian et al., 2011)), fewer studies look at the shape and dynamics of the decline phases, which can provide important hints regarding the effect of interactions on the process of microbial mortality (e.g. (Christie-Oleza et al., 2017; Grossart, 1999; Ratzke & Gore, 2017)).

Here, we explore to what extent intra-clade diversity affects the outcome of microbial interactions, using growth curves as the major phenotypic "readout". Our model organisms are two globally abundant clades of marine bacteria: a cyanobacterial primary producer (*Prochlorococcus*) and a heterotrophic γ-proteobacterium (*Alteromonas*). Interactions between marine phototrophs (phytoplankton, including cyanobacteria) and heterotrophic bacteria have been studied intensively, as phytoplankton are responsible for about one-half of the photosynthesis on Earth (e.g. (Cirri & Pohnert, 2019; Cole, 1982; Field et al., 1998; Ramanan et

al., 2016; Seymour et al., 2017)). Thus, phytoplankton-bacteria interactions may strongly affect community structure and function on scales from microns to thousands of kilometers (Hennon et al., 2018; J. Jeffrey Morris et al., 2012). Our model primary producer, *Prochlorococcus*, is found throughout the euphotic zone, the sunlit upper portion of the ocean. There are multiple *Prochlorococcus* clades, broadly partitioned into high-light (HL) and low light (LL) adapted ecotypes, which differ in their photosynthetic parameters and occupy different niches in the ocean (surface vs deep water, reviewed by (Biller et al., 2015)). Strains differ also in traits such as the capacity to utilize different forms of inorganic nutrients and organic matter, as well as in their interactions with heterotrophic bacteria and phage. *Alteromonas* is a clade of free-living marine bacteria, which are also partitioned into surface and deep groups (*A. macleodii* and *A. mediterranea*, respectively) (López-Pérez & Rodriguez-Valera, 2016). *Alteromonas* strains also exhibit diverse capabilities to utilize carbohydrates, acquire iron and in motility (Koch et al., 2020). Interactions between individual strains of *Prochlorococcus* and *Alteromonas* have been characterized in some detail (Aharonovich & Sher, 2016; Diner et al., 2016; Hennon et al., 2018; Hou et al., 2018; J. J. Morris et al., 2011; Roth-Rosenberg et al., 2020; Sher et al., 2011). While the phenotype and gene expression patterns during interactions vary between strains, this variability has not been explored systematically (Aharonovich & Sher, 2016; Biller et al., 2016; Sher et al., 2011). Notably, strain- and condition-dependent phytoplankton-heterotroph interactions are observed also in other systems, including *Synechococcus*, a close relative of *Prochlorococcus* (Christie-Oleza et al., 2017; Zheng et al., 2020), as well as eukaryotic microalgae (e.g. coccolithophores and diatoms, (Amin et al., 2015; Grossart & Simon, 2007; Segev et al., 2016; Seyedsayamdost et al., 2011)).

We characterized the interactions between five strains each of *Prochlorococcus* and *Alteromonas*, from the first encounter between previously-axenic strains (i.e., grown in mono-culture) and over up to 435 days of co-culture (25 phototroph-heterotroph combinations across ~1.2 years, Figure 1a, Figure 1–figure supplement 1). The culturing period spanned multiple cycles of exponential growth, culture decline and long-term nitrogen starvation (Roth-Rosenberg et al., 2020). Nitrogen stress or starvation occurs across wide swaths of the global ocean, and affects a significant fraction of the *Prochlorococcus* diversity (Saito et al., 2014; Ustick et al., 2021). We focused our analysis on *Prochlorococcus* growth and decline, which is easily measured using bulk culture fluorescence in a non-invasive manner (e.g. (Coe et al., 2016; Sher et al., 2011). Using this dataset of 429 growth curves, as well as associated cell number measurements and genome resequencing, we ask: i) How do the interactions between *Prochlorococcus* and *Alteromonas* vary across the diversity of each organisms? ii) Do the interactions change over time (i.e. do the organisms adapt to "living together")? iii) When, during the life-cycle of a *Prochlorococcus* batch culture, do microbial interactions have the largest impact on growth and death, and can this impact be quantified? iv) Can the combination of growth curves, cell counts and genomic data provide hints as to which potential metabolic pathways are affected by the long-term interactions?

Results and Discussion

Differences in co-culture phenotype are related to *Prochlorococcus* but not *Alteromonas* strains

The axenic cultures and the co-cultures differed primarily in their decline stage, and this was observed already from the first encounter between previously-axenic *Prochlorococcus* and *Alteromonas* (Experiment 1). In experiment 1, all co-cultures and axenic controls grew exponentially (Figure 1a, b). However, all axenic cultures showed a rapid and mostly monotonic decrease in fluorescence starting shortly after the cultures stopped growing, reaching levels below the limit of detection after ~20-30 days. In contrast, the decline of co-cultures rapidly slowed, and in some cases was interrupted by an extended "plateau" or second growth stage (Figure 1b). Across multiple experiments, 92% of the co-cultures contained living cells for at least 140 days, meaning that they could be revived by transfer into fresh media. In contrast, none of the axenic cultures were able to re-grow when transferred into fresh media after 60 days (Figure 1a, Figure 1–figure supplement 1). These results are consistent with previous studies of *Prochlorococcus* (Roth-Rosenberg et al., 2020) and *Synechococcus* (Christie-Oleza et al., 2017). Similarly, it has previously been shown that *Prochlorococcus* MIT9313 is initially inhibited by co-culture with *Alteromonas* HOT1A3, while MED4 is not (Aharonovich & Sher, 2016; Sher et al., 2011). This "delayed growth" phenotype was observed here too, was specific to MIT9313 (not observed in other *Prochlorococcus* strains) and occurred with all *Alteromonas* strains tested (Figure 1b).

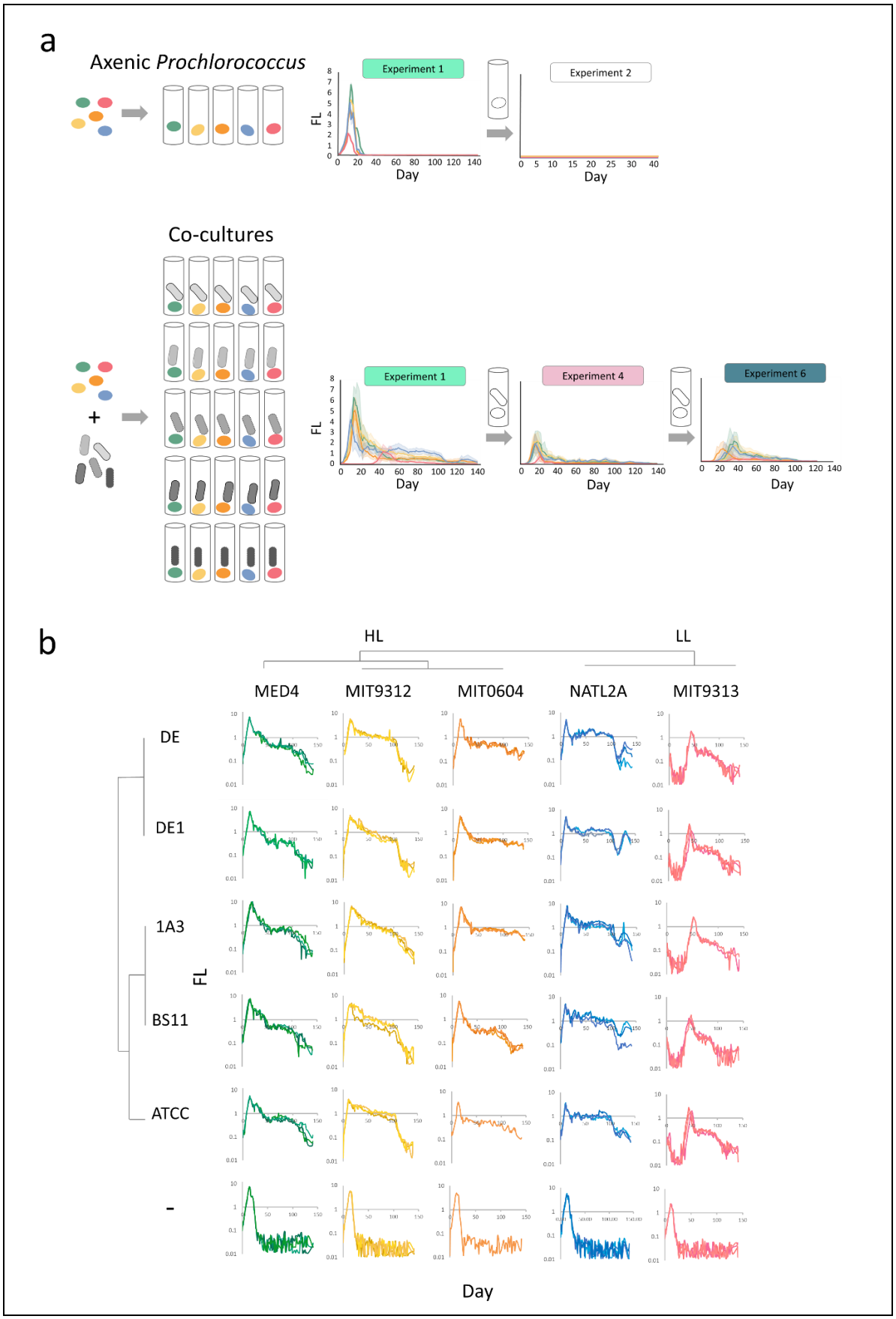
a
Axenic Prochlorococcus
Experiment 1
Experiment 2
FL
Day
Co-cultures
Experiment 1
Experiment 4
Experiment 6
FL
Day
b
HL
LL
MED4
MIT9312
MIT0604
NATL2A
MIT9313
DE
DE1
1A3
BS11
ATCC
-
FL
Day

Figure 1: Overview of the dynamics of *Prochlorococcus-Alteromonas* co-cultures from first encounter and over multiple transfers. a. Mean growth curves of the five *Prochlorococcus* strains over multiple cycles of exponential growth, culture decline and long-term starvation. The top row shows the transfer of axenic strains from experiment 1 after 60 days, with no subsequent growth observed. The bottom row shows the transfer of co-cultures from experiment 1 after 100 days (experiment 4) and additional transfer after 140 days (experiment 6), with subsequent growth. Shaded areas indicate standard error. b. High reproducibility and strain-specific dynamics of the initial contact between *Prochlorococcus* and *Alteromonas* strains (experiment 1). Three biological replicates for each mono-culture and co-culture are shown.
Figure 1 – figure supplement 1: Flowchart of the experimental procedure.
Figure 1 – figure supplement 2: Differences in growth between first experiment and subsequent transfers.

140

141 A visual inspection of the growth curves in Figure 1b suggested subtle yet consistent differences
142 in the shape of the growth curve, and especially the decline phase, between different
143 *Prochlorococcus* strains. To test this, we used the growth curves as input for a Principal
144 Component Analysis (PCA), revealing that the growth curves from each *Prochlorococcus* strain
145 clustered together, regardless of which *Alteromonas* strain they were co-cultured with (Figure 2).
146 The growth curves of all high-light adapted strains (MED4, MIT9312 and MIT0604) were relatively
147 similar, the low-light I strain NATL2A was somewhat distinct, and the low-light IV strain MIT9313
148 was a clear outlier, consistent with this strain being the only one initially inhibited in all co-
149 cultures. This strain (MIT9313) stands out even when the impact of growth timing and magnitude
150 was removed by performing the ordination after scaling and aligning the growth times. The
151 survival of *Prochlorococcus* after extended nitrogen starvation and the clustering of the growth
152 curves by *Prochlorococcus* but not *Alteromonas* strains were observed also in multiple subsequent
153 transfers into fresh media, and are thus robust to the time in co-culture and the initial cell
154 densities (Supplementary text).

155 MIT9313 belongs to the low-light adapted clade IV (LLIV), which are relatively distant from other
156 *Prochlorococcus* strains and differ from them in multiple physiological aspects including the
157 structure of their cell wall (Ting et al., 2007), the use of different (and nitrogen-containing)
158 compatible solutes (Klähn et al., 2010) and the production of multiple peptide secondary
159 metabolites (lanthipeptides,(Cubillos-Ruiz et al., 2017; Li et al., 2010)). LLIV cells also have larger
160 genomes, and are predicted to take up a higher diversity of organic compounds such as sugars
161 and amino acids (Yelton et al., 2016). It is intriguing that this strain, which has higher predicted
162 metabolic and regulatory flexibilities (Kettler et al., 2007), differs from all other *Prochlorococcus*
163 strains in the phenotype of co-culture and is the only one initially inhibited in co-culture with
164 *Alteromonas*.

165

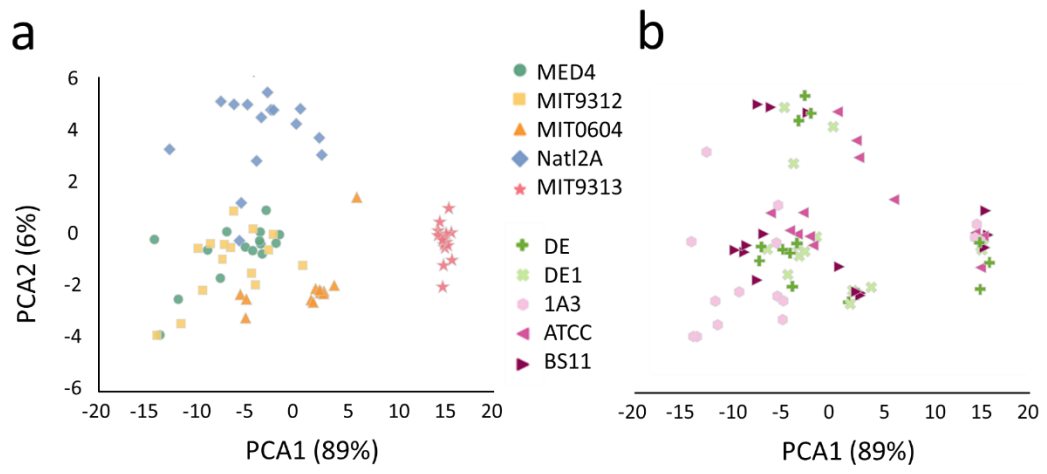

Figure 2: Principal component analysis (PCA) of the growth curves from all co-cultures during 140 days of experiment 1. The ordination is colored by *Prochlorococcus* (a) and by *Alteromonas* (b) strains. The growth curves cluster by *Prochlorococcus* strain (Adonis test, F(4,68) = 80.425, p = 0.001) and not by *Alteromonas* strain (Adonis test, F(4,68) = 1.69, p = 0.17)
Figure 2 - figure supplement 1: PCA of the growth curves from experiments 3-6.
Figure 2 - figure supplement 2: Classification of Prochlorococcus strains and identification of important culture stages differentiating between strains using machine learning.

The differences between *Prochlorococcus* strains are most evident in the decline and long-term starvation stages

We next used Random Forest Classification to quantitatively determine which stages of the co-culture were most different between the *Prochlorococcus-Alteromonas* pairs. The algorithm accurately predicted, from the growth curves, the *Prochlorococcus* strain (10x cross validation accuracy 0.92±0.17). However, it performed much more poorly when trying to predict the *Alteromonas* strain (accuracy 0.62 ± 0.58) (Figure 2 - Figure supplement 2a), providing further support to the observation from the PCA in Figure 2 that the shape of the growth and decline curves was driven by the specific *Prochlorococcus* strain and not by the *Alteromonas*. The classification of the *Prochlorococcus* strains relied heavily on days during the decline phase, as these times had the highest Random Forest feature importance, in agreement with the visual inspection of the growth curves (Figure 2 - Figure supplement 2b). Similar results were obtained in all subsequent transfers (Supplementary text, Figure 2 - figure supplement 2a).

Focusing on the decline stage, we asked whether the differences in growth curves during long-term co-culture represent differences in the number of cells. This is because physiological differences such as in the amount of chlorophyll per cell, or the fraction of chlorotic *Prochlorococcus* cells, could also affect the growth curves (Coe et al., 2016; Roth-Rosenberg et al., 2020). Flow cytometry counts during the decline stage (after 60, 100 and 140 days) revealed a decrease in the number of *Prochlorococcus* cells over time (Figure 3a), yet the number of cells in

the co-cultures was still 3-4 orders of magnitude higher than in the axenic cultures (Figure 3 - Figure supplement 1). This is consistent with the growth curves (Figure 1). The number of *Alteromonas* cells also declined with time in the co-cultures (Figure 3a), but the difference between the axenic cultures and the co-cultures was much less pronounced than in *Prochlorococcus* (up to ~4-5-fold after 100 days, Figure 3 - Figure supplement 1c). This may be due to the ability of *Alteromonas* to utilize the organic carbon from the natural-seawater-based media, in addition to the dissolved organic matter (DOM) produced by *Prochlorococcus* (Pedler et al., 2014).

We next asked whether the carrying capacity of the long-term co-cultures, defined as the sum of the concentrations of *Prochlorococcus* and *Alteromonas* cells, depends on the *Prochlorococcus* or the *Alteromonas* strain. Put differently, one could hypothesize that the total number of cells (and hence the carrying capacity) of the co-culture could depend on the photosynthetically-fixed C provided by *Prochlorococcus*, or alternatively on the recycling capacity of the different *Alteromonas* strains. As shown in Figure 3b and 3c, on days 60 and 100, the number of both *Prochlorococcus* and *Alteromonas* cells clustered depending on the *Prochlorococcus* strain (Adonis, $p = 0.001$), but not on the *Alteromonas* strain (Adonis, $p>0.05$). In terms of carrying capacity, there are clear differences between *Prochlorococcus* strains (Figure 3 - Figure supplement 2a), but not *Alteromonas* strains (Figure 3 - Figure supplement 2b). Interestingly, two of the *Prochlorococcus* strains, MIT9312 and MIT9313 have similar (and lower) carrying capacity. These two strains belong to different ecotypes but were isolated from the same drop of water. Taken together, these results suggest that it is the dynamics of the *Prochlorococcus* strains, including potentially the amount or composition of fixed and released organic C, which determine the total community carrying capacity.

By day 140, the cell numbers had declined significantly, and there was no longer a correlation between the number of *Prochlorococcus* and *Alteromonas* cells (Figure 3). This suggests that the system is not in steady state, with a slow yet constant reduction in carrying capacity evident by the decrease in cell numbers. Indeed, the co-cultures did not survive indefinitely - in a subsequent experiment, only 16/30 cultures could be transferred after 195 days (Figure 3 - Figure supplement 3a, b), and only 3/75 cultures could be transferred after 250 days (Figure 3 - Figure supplement 3c). Notably, MIT0604 was the strain most likely to survive transfer after these extended periods, and was also the most abundant strain after 140 days (Figure 3b). While we do not currently have an explanation for the higher survival of this strain, it is noteworthy that it is the only strain to utilize nitrate (Hackl et al., 2021).

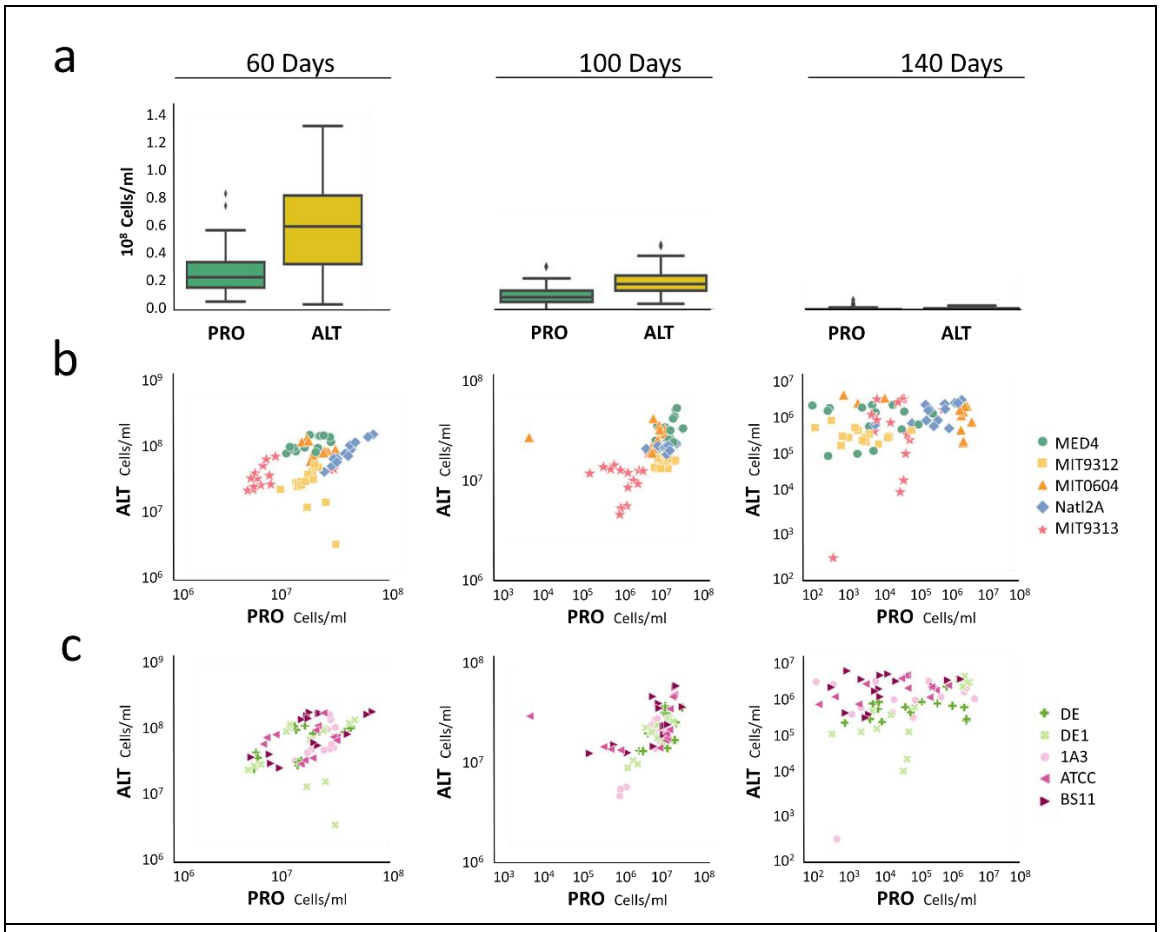

Figure 3: *Prochlorococcus* strain determines the cell numbers of the co-cultures at long term starvation. a. Total co-cultures cell numbers at three different time points, showing a gradual decline. b. *Prochlorococcus* and *Alteromonas* cell numbers, colored by *Prochlorococcus* strain and by *Alteromonas* strain (c) at each time point. Note the clustering of samples based on *Prochlorococcus* but not *Alteromonas* after 60 and 100 days, but not after 140 days.
Results of Adonis test for *Prochlorococcus*:
day 60: $F(4,68) = 32.99$, $p = 0.001$
day 100: $F(4,68) = 28.73$, $p = 0.001$
day 140: $F(4,68) = 16.69$, $p = 0.001$
Results of Adonis test for *Alteromonas*:
day 60: $F(4,68) = 1.599$, $p = 0.149$
day 100: $F(4,68) = 1.998$, $p = 0.074$
day 140: $F(4,68) = 2.212$, $p = 0.043$

Figure 3 – figure supplement 1: carrying capacity of the mono-cultures (axenic *Prochlorococcus*) and co-cultures
Figure 3 - figure supplement 2: Carrying Capacity of the co-cultures per strain
Figure 3 - figure supplement 3: Some co-cultures are able to survive for extended periods (>195 days).

220

221

Modeling the effect of co-culture on *Prochlorococcus* mortality

Given that the most striking effect of co-culture was on the decline phase of the co-cultures, we asked whether we could quantify this effect, and whether we could identify an appropriate model for mathematically describing culture decline. Importantly, while the growth of bacteria has been extensively studied and modelled, the decline of bacterial cultures, representing bacterial mortality, is much less studied, and mortality is rarely represented in ecological or biogeochemical models of microbial dynamics (Shoemaker et al., 2021). Bacterial mortality has, however, often been modelled in the context of food safety and genome evolution, using either mechanistic or descriptive approaches (Brouwer et al., 2017; Crane & Moore, 1986; Finkel & Kolter, 1999; Patra & Klumpp, 2013; Shoemaker et al., 2021) We chose to focus on four previously-described models which are relatively simple and have a clear biological interpretation (Figure 4a, Table 1). The Exponential model is the simplest and most commonly used one (Pruitt & Kamau, 1993). The Bi-exponential model is slightly more complex, representing two separate subpopulations in the community, each with its own death rate (Crane & Moore, 1986). Weibull model is a probabilistic model, modeling heterogeneous population with a diverse stress tolerance (Shoemaker et al., 2021; Van Boekel, 2002) and finally the Harmonic model employs a quadratic rate of decline which is often associated with predator-prey interaction or encounter rate (Pruitt & Kamau, 1993). When fitting each of these models to the decline phase of the growth curves, the Weibull model stands out as it has a low error for both axenic and co-cultures (Table 1, Figure 4b). Based on this model, and assuming that culture fluorescence is related to the number of non-lysed cells in the media, axenic *Prochlorococcus* cells die more than ten-fold faster than cells in co-culture (2-decimal reduction time, td_2, is 12.58 ± 3.85 days for axenic cultures and 316 ± 337 days for co-cultures).

Table 1: Mathematical description and biological interpretation of four models used to describe bacterial mortality

Mathematical model	Derivative	# Params[1]	Physiological Interpretation	Axenic RMSE [2] (n=13)	Co-culture RMSE (n=343)	Reference
Exponential $X = X_0\, e^{-a\,t}$	$\frac{dX}{dt} = -aX$	1	Constant ratio of the population dies in each time point	0.26 ± 0.11	0.29 ± 0.21	(Pruitt & Kamau, 1993)
Bi-Exponential $X = X_0(f\, e^{-a_1\,t} + (1-f)\, e^{-a_2\,t})$	$\frac{dX}{dt} = -f a_1 X_1 - (1-f)\, a_2 X_2$	3	Two subpopulations with different persistence under stress and death rates	0.26 ± 0.11	0.16 ± 0.12	(Crane & Moore, 1986)
Harmonic $X = X_0\, \frac{1}{1+a\,t}$	$\frac{dX}{dt} = -a\, X^2$	1	Quadratic mortality rate – dependence on cell-cell encounters	0.50 ± 0.19	0.19 ± 0.13	(Pruitt & Kamau, 1993)
Weibull $X = X_0\, e^{-\frac{t^n}{a}}$	$\frac{dX}{dt} = -c\, t^{n-1} X *$	2	Probabilistic model with a heterogeneous distribution of stress tolerance	0.14 ± 0.08	0.18 ± 0.11	(Van Boekel, 2002)

[1] # Params – number of free parameters

[2] RMSE - Root Mean Square Error

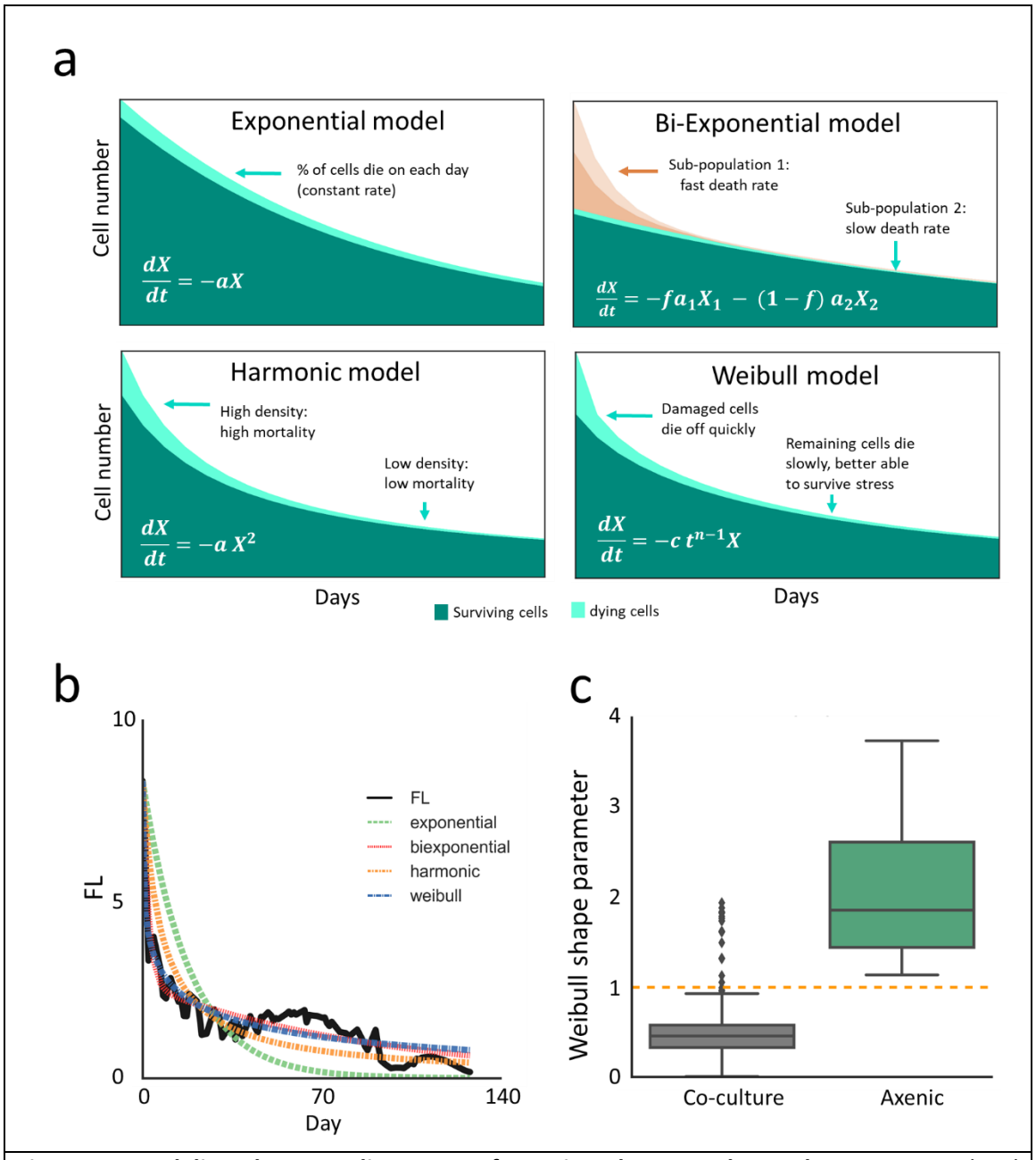

Figure 4: Modeling the mortality stage of axenic cultures and co-cultures. a. Graphical representation of four decline models. The lighter blue or peach colors represent the dying fraction of the population at each time-point. b. Comparison of the four decline models with co-culture of *Prochlorococcus* NATL2A with *Alteromonas* HOT1A3. While the Weibull model provides the best fit (see Table 1), none of the decline models fully describes the complexities of culture decline. c. Weibull Shape parameter (n) in co-cultures vs axenic cultures (student t-test, $p < 0.001$). In all axenic samples $n>1$, and hence the decline rate increases over time. In most co-cultures $n<1$, suggesting that, as the culture declines, the remaining cells are better adapted to stress and thus their death rate decreases.

249

In the Weibull model, the 'shape parameter' (n) represents the change over time in the susceptibility of the bacterial community to stress. A shape parameter above one represents an increasing probability that cells will die as time increases (e.g. due to the accumulation of damage), whereas a shape parameter below one suggests that, over time, the cells become more resistant to damage. Axenic cultures have high shape value of 2.1 ± 0.9, suggesting an accumulation of cell damage leading to increasing death rate, whereas that of co-cultures is 0.5 ± 0.3 (student t-test, $p < 0.001$) (Figure 4c). This suggests that, in contrast to mono-cultures, in each cycle of co-culture the *Prochlorococcus* cells are acclimating over time to the nutrient stress conditions.

While the Weibull model is useful in quantifying mortality rates and raising the hypothesis that *Prochlorococcus* cells are acclimating to starvation over time, none of the tested models was able to fully capture the intricate dynamics of culture decline (Figure 4b). In most co-cultures involving *Prochlorococcus* strains NATL2A, MED4 and MIT0604, culture decline was not monotonic, and was interrupted by a second growth phase about 40-50 days after the cultures started declining. We propose that this "second breath" represents either a consistent shift in the physiology of one of the interacting partners (e.g. by activating pathways for the salvage of previously-exuded DOM) or a change in the availability of labile DOM, e.g. following a period of mortality and lysis of *Prochlorococcus* and/or *Alteromonas*. Because the second growth phase was mostly absent in MIT9312 and MIT9313, we speculate that this phenomenon, too, is driven primarily by the specific strain of *Prochlorococcus* cells in co-culture. Notably, the Weibull model, while best representing the experimental results, is less appropriate for ecological/biogeochemical models, because the time from peak is an inherent part of the differential equation. In such cases, the harmonic model formulation may be more appropriate, as it represents mortality of co-cultures better than exponential decline with the same number of parameters, and quadratic expressions for mortality are already used in such models (Dutkiewicz et al., 2001; S. K. Moore et al., 2006; Murray A.G. and Parslow J.S., 1999).

Accumulated mutations in *Prochlorococcus* suggest a role for nitrogen use and the stringent response

During the experiments described above, we co-cultured strains of *Prochlorococcus*, which had each been previously maintained in axenic mono-cultures for hundreds or thousands of generations. We also exposed these parental strains, which are routinely maintained under conditions of exponential growth, to repeated cycles of growth, mortality and long-term survival under N starvation. To identify whether these shifts in life-style could result in genetic changes in the co-cultured populations, we re-sequenced the genomes of duplicate cultures of *Prochlorococcus* MIT9313 co-cultured with *Alteromonas* HOT1A3 after a total of 435 days in co-culture (including 3 cycles of growth, mortality and survival, Figure 5a, Figure 1 – figure supplement 1). We also re-sequenced the parental strain used in these experiments, which itself had been maintained as an axenic culture for ~16 years since originally being sequenced (Rocap et al., 2003). Since the read coverage for *Alteromonas* was low, we focus here on *Prochlorococcus*.

290 Over the course of 435 days in co-culture (~220 generations), the two replicate MIT9313 co-
291 cultures accumulated 32 and 39 observed mutations in protein-coding genes, compared to 57
292 mutations accumulated in the parental strain over ~16 years of growth at similar maximum
293 population sizes (~2,900 generations, 15-20ml cultures, Figure 5, Figure 5- Figure supplement 1
294 and Figure 5 - source data 1). This suggests that, during the repeated cycles of growth, decline
295 and starvation, the mutation rate of MIT9313 in co-culture increased roughly 7-9-fold compared
296 to the parental axenic strain growing primarily exponentially (Supplementary text). Strikingly,
297 many of the mutations were observed to occur in genes involved in nitrogen utilization and stress
298 responses. Three genes involved in nitrogen metabolism each had two or more mutations
299 associated with them – the nitrite reductase gene nirA and two genes in the operon involved in
300 the production and transport of glycine betaine (Figure 5b, c).

301 The parental MIT9313 strain had a frameshift mutation in the N'-terminal reductase domain of
302 nirA, observed in 100% of the sequencing reads, which likely led to a truncated, inactive protein.
303 This frameshift is not found in the evolved strain, after ~220 generations in co-culture. Since nitrite
304 was not added to the (co)-cultures, and the *Alteromonas* genome does not contain the genes for
305 nitrification (the ammonia monoxygenase gene), this raises the question of what are the sources
306 of nitrite that is presumably being utilized by the evolved strain. We provide a speculative answer
307 in Figure 5d. It has previously been shown, in the freshwater cyanobacterium *Phormidium*, that
308 nitrite can be produced by the enzymatic dismutation of hydroxylamine (NH_2OH) in the presence
309 of hydrogen peroxide, H_2O_2 (reaction 3 in Figure 5d, the other product is NH_3 (Bagchi & Kleiner,
310 1990, 1991)). NH_2OH, in turn, can be produced by the peroxidation of glutamine to glutamate
311 (reaction 2 in Figure 5d, (Bagchi & Kleiner, 1991)). The H_2O_2 required for these reactions is
312 produced by multiple metabolic reactions in cyanobacteria (Latifi et al., 2009), and it has
313 previously been shown that oxidative stress is enhanced during nitrogen starvation in
314 *Prochlorococcus* (Mcdonagh et al., 2012). Thus, an active nitrite reductase may enable MIT9313
315 to recycle NH_2OH, produced when the cells are under nitrogen starvation conditions (Figure 5d).
316 Intriguingly, H_2O_2 is also produced during amino acid oxidation, the process in which cells degrade
317 amino acids to obtain N and carbon backbones (e.g. by several types of L-amino acid oxidases,
318 reaction 1 in Figure 5d, (Schriek et al., 2007)). It is currently unclear to what extent these amino
319 acid degradation pathways are present and active in *Prochlorococcus*, as the streamlined
320 genomes of these organisms lack several known enzymes (Gau et al., 2007; Schriek et al., 2007),
321 although we note that a putative L-aspartate oxidase had a non-synonymous mutation in the
322 evolved strains. If, however, nitrogen starvation induces amino acid oxidation and the production
323 of H_2O_2 in *Prochlorococcus*, this would provide a mechanistic explanation for the inability of these
324 organisms to survive long-term N starvation alone (J. Jeffrey Morris et al., 2008, 2012) Further
325 studies are required to test this hypothesis.

326 Three genes in the operon for the production and import of the compatible solute glycine betaine
327 accumulated mutations – the glycine-sarcosine methyltransferase *gsmt*, and two subunits of the
328 glycine-betaine ABC transporter (Figure 5c). None of the mutations occurred in residues known
329 to be important to the activity of these proteins. Under N starvation, it is possibly advantageous
330 for the cells to reduce the production of glycine betaine, which contains N atoms, in favor of other
331 compatible solutes such as sucrose (Klähn et al., 2010). However, during the long experiments
332 described here, it is also likely that the osmotic strength of the growth media increased (due to

333 both cell lysis and the evaporation of water), and this could lead to an increased requirement for
334 glycine betaine (Klähn et al., 2010). Further work is needed in order to differentiate between these
335 two hypotheses. Importantly, glycine betaine provides both carbon (energy) and N to co-occurring
336 bacteria, including SAR11 (Becker et al., 2019). Additional genes involved in N metabolism that
337 accumulated non-synonymous mutations (one for each gene) include enzymes involved in amino
338 acids production or degradation (the L-aspartate oxidase mentioned above, biosynthetic arginine
339 decarboxylase and cysteine synthase) and a putative aminotransferase (Figure 5b, Figure 5 -
340 Source Data 1). Genetic changes occurred in additional genes not directly related to nitrogen
341 metabolism, but known to be involved in the nitrogen stress response in cyanobacteria. These
342 include the glycogen synthase gene glgA (Tolonen et al., 2006) as well as genes involved in the
343 synthesis of chlorophyll and other proteins from the photosynthetic apparatus.

344 Finally, the bacterial "alarmone" (p)ppGpp is a master regulator of bacterial stress responses,
345 including the "stringent response" to carbon or amino acid starvation (recently reviewed by
346 (Steinchen & Bange, 2016)). Two mutations were observed in a gene homologous to the relA/spoT
347 bifunctional (p)ppGpp synthase/hydrolase. The product of this gene both activates the stringent
348 response by synthesizing (p)ppGpp from GTP and represses it, by hydrolyzing the alarmone back
349 to GTP (Hogg et al., 2004; Steinchen & Bange, 2016). Both of the mutations were in the hydrolase
350 domain, and one of them (P95T) occurs in a residue which is predicted to take part in Mn
351 coordination in the active site of the enzyme, potentially leading to a hydrolase-incompetent
352 enzyme (Hogg et al., 2004; Steinchen & Bange, 2016). We speculate that this mutant may be
353 deficient in its ability to "turn off" the stringent response, potentially leading to enhanced survival
354 under stress.

355

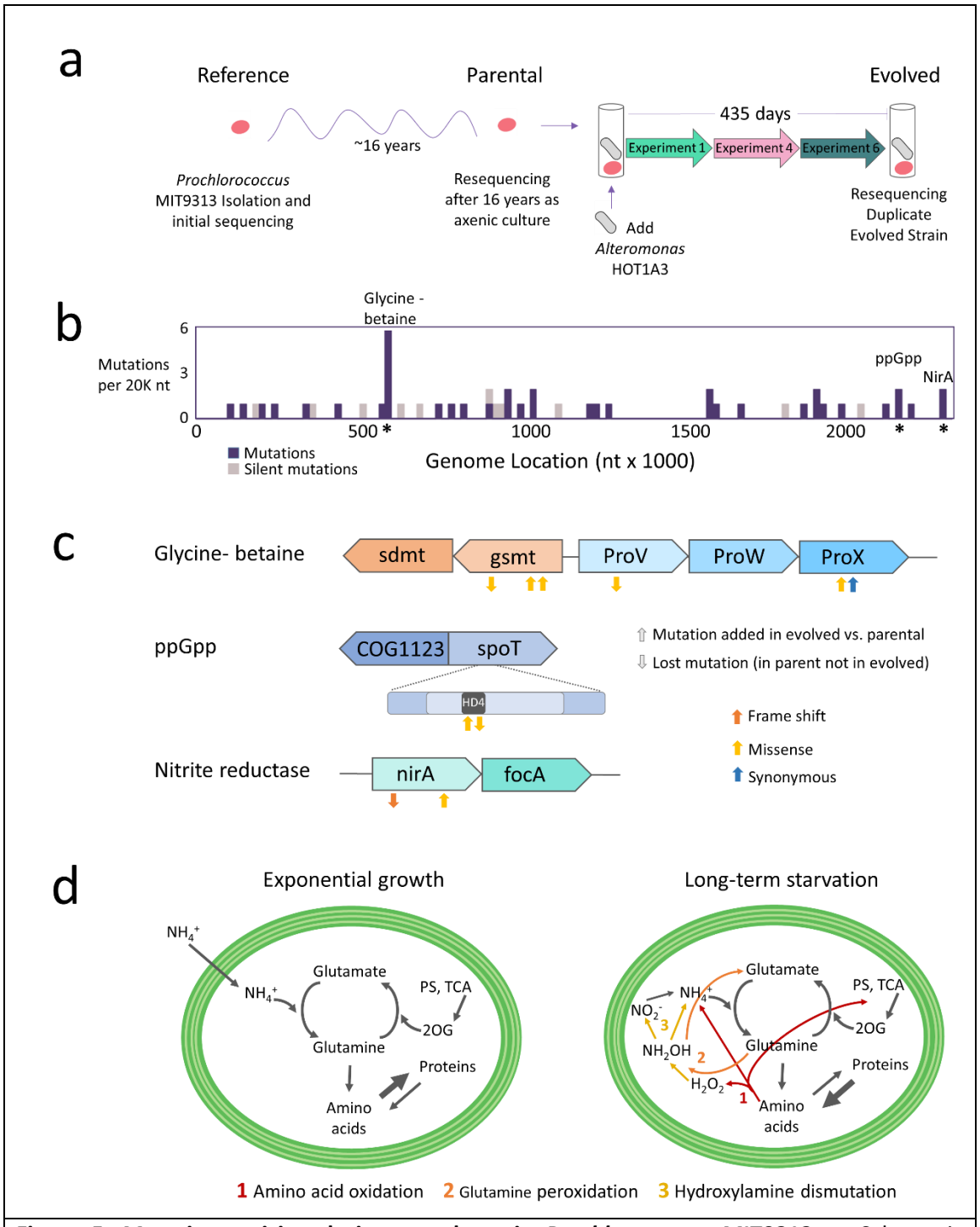

Figure 5: Mutations arising during co-culture in *Prochlorococcus* MIT9313. a. Schematic illustration of resequencing setup. b. Location of accumulated mutations (SNPs or indels) on the MIT9313 genome. Bars represent the number of mutations (changes between the parental and evolved populations) per 20,000 bases in both biological duplicates. Dark purple bars represent non-synonymous mutations; light grey bars represent synonymous mutations. c. Type and location of mutations in genes involved in Glycine-betaine, ppGpp and Nitrite reductase metabolism. The bar below the spoT gene shows the domain structure. d. Schematic diagram of the proposed role of nitrite reductase during long-term starvation in MIT9313. The

suggested pathway leading to the production of nitrite (NO_2^-) through hydroxylamine (NH_2OH) is shown in long term starvation compared to exponential growth. The balanced equations for this pathway are: Reaction 1 - amino acid oxidation by L-amino acid oxidases (e.g. Alanine + H_2O + O_2 -> Pyruvate + NH_4^+ + H_2O_2); Reaction 2 - Peroxidation of glutamine to glutamate ($C_5H_{10}N_2O_3$+H_2O_2->$C_5H_9NO_4$ + NH_2OH); Reaction 3 - Dismutation of hydroxylamine in the presence of H_2O_2 (2NH_2OH + H_2O_2 -> NO_2^- + NH_4^+ + 2H_2O). PS – photosynthesis, TCA - tricarboxylic acid cycle, 2OG - 2-oxoglutarate

Figure 5 - figure supplement 1**:** Location of mutations in the parental strain (after ~16 years of culture transfers)

Figure 5 - Source Data 1: Mutations in resequencing of *Prochlorococcus* MIT9313 after co-culturing with *Alteromonas* HOT1A3

Summary and future directions

As our appreciation of the richness and dynamicity of microbial communities increases, so does the understanding that interactions between microorganisms are critical to the structure and function of these communities. Elucidating the roles of microbial interactions requires both well-characterized model organisms and a way to extend the insights from such models across the diversity of organisms and environmental conditions. Our results from the highly-simplified system of multiple *Prochlorococcus* and *Alteromonas* strains provide an important step towards this goal. Using the rich information on interaction phenotypes present in the growth and decline curves, we identify conserved and strain-specific facets of these interactions. Despite the genetic diversity across the *Alteromonas* strains studied, it was the identity of the *Prochlorococcus* strain that determined the interaction phenotype. This manifests in the growth and decline rates, in the shape of the curve (primarily the decline phase), and in the number of cells living in long-term, nitrogen-starved co-culture. Testing multiple mathematical models of culture decline suggests that cells in axenic cultures are accumulating damage and dying more rapidly over time, while cells in co-culture are acclimating, likely changing their physiology and also evolving to better deal with the emergent stress. Comparing the modelled and observed curves allows for the identification of consistent and reproducible shifts in physiology, for example the “second breath” of growth followed by rapid decline in NATL2A co-cultures (Figure 4b), that can then be studied in-depth.

Under our laboratory conditions, it is likely that nitrogen starvation is the main selection force driving the phenotypic outcome of long-term co-cultures, although other stressors such as the increase in osmolarity/salinity or the accumulation of waste products cannot be ruled out. We speculate that the genetic changes observed in the MIT9313 population are primarily indicative of processes occurring in the *Prochlorococcus* cells due to nitrogen starvation and/or osmotic stress, rather than representing a direct response to the interactions with *Alteromonas*. It is possible that a major effect of co-culture with *Alteromonas* is to slow down the deterioration in *Prochlorococcus* homeostasis, providing a “buffer” that enables *Prochlorococcus* to activate its own starvation survival responses, and subsequently to genetically evolve. *Alteromonas* may similarly allow *Prochlorococcus* to adapt to light starvation (Coe et al., 2016), yet the genetic mechanisms underlying this survival remain unclear (Coe et al., 2020). However, the buffering

effect of *Alteromonas* cannot be taken for granted, as it also depends on culture conditions, for example CO_2 concentrations (Hennon et al., 2018).

Once mortality has been slowed down enough to allow acclimation and/or adaptation, the differences in the resulting shape of the co-culture curves are likely due to strain-specific differences in nitrogen metabolism. For example, *Prochlorococcus* MIT9313 produces glycine betaine as a compatible solute (unlike MIT9312 and NATL2A (Klähn et al., 2010)), and it is possible that producing large amounts of this N-containing molecule constrains the metabolic responses of this strain to N starvation differently from other strains, resulting in this strain having a distinct phenotype. The reasons for the differences between the other *Prochlorococcus* strains are less clear, but may be related to differences in the regulatory networks (e.g. those affected by the ppGpp alarmone) or the capacity to utilize organic substances released by *Alteromonas* (Yelton et al., 2016). Some of the mutations were in hypothetical genes and in some cases in multiple hypothetical genes in the same putative operon (e.g. PMT1541 and PMT1542). Future work is needed to determine whether these represent "internal" *Prochlorococcus* processes, or whether they are part of the tools used by *Prochlorococcus* to interact with co-occurring bacteria.

Why is it the identity of the primary producer (*Prochlorococcus*) rather than the heterotrophic "recycler" (*Alteromonas*) that determines the outcome of the co-culture? *A-priori*, it was reasonable to assume that the co-culture phenotype would be affected by the differences between the *Alteromonas* strains in their ability to degrade and utilize polysaccharides and a variety of other organic molecule (Koch et al., 2019, 2020). We speculate that the growth of *Alteromonas* in the co-cultures is fueled primarily by the availability of major biomass components released by *Prochlorococcus* as they die, such as proteins, amino acids and nucleotides. Such common macromolecules do not require highly specialized metabolic processes to degrade and utilize, and hence could be utilized by all of the *Alteromonas* strains. It is possible that the differences between *Alteromonas* strains may manifest when more complex macromolecules are available, e.g. from plant material, or when all of the "easy to digest" (labile) organic matter has been utilized and only complex macromolecules remain (Teeling et al., 2012). These conditions may not have been met in our experiments. Regardless of the underlying mechanism, identifying to what extent the interaction phenotype is dependent on the identity of each of the interacting organisms requires an experimental setup spanning the diversity of both.

Our results identify patterns in the interactions between clades of abundant marine phototrophs and heterotrophs, including consistent shifts in physiology occurring after extended time in co-culture. The mechanistic basis of these shifts in physiology can now be studied in-depth. Given that these shifts occur under conditions where nutrients are scarce and their availability likely depends on recycling between phototrophs and heterotrophs, it is tempting to speculate that such mechanisms may be physiologically relevant in the oligotrophic ocean, much of which is N-stressed (Ustick et al., 2021). Nevertheless, the co-cultures did not reach a steady state, and did not represent a closed system. Thus, processes not represented in these simplified laboratory co-cultures, are necessary to explain the long-term stability over decades of *Prochlorococcus* in the oceans (Malmstrom et al., 2010). Such processes could include multi-organism interactions, as natural communities are much more complex than the laboratory co-cultures, as well as oceanographic processes such as nutrient injection through deep mixing. More generally, cell mortality is intimately linked with the amount and type of recycled organic matter, yet the rate

of mortality in natural communities is highly unconstrained (Beckett et al., 2021). Hence, better representation of mortality in mathematical models (e.g. the use of appropriate mortality formulations) is likely important for understanding biogeochemical cycles (Beckett et al., 2021). Finally, this study is a reminder that bacterial growth curves represent an information-rich representation of the life and death of cells, which can be mined to identify potential physiological changes of ecological relevance.

Materials and Methods

Strains and experiment set up

Axenic *Prochlorococcus* strains MED4, MIT9312, MIT0604, Natl2A and MIT9313 were maintained in Low N Pro99 media, based on natural sea water, with the addition of 100 µM nitrogen, 50 µM phosphorus and trace metal elements. Under these conditions, *Prochlorococcus* enter stationary stage due to the depletion of NH_4 from the media and nitrogen starvation (Grossowicz et al., 2017). *Alteromonas* strains HOT1A3, Black sea 11, ATCC27126, AltDE1 and AltDE were maintained in ProMM media. both under constant cold while light (27 $\mu Em^{-2} s^{-1}$) at 22ºC in (L. R. Moore et al., 2007; Sher et al., 2011)). Prior to the experiment, the axenicity of the *Prochlorococcus* cultures was tested by inoculating 1 ml culture into 15 ml ProMM (L. R. Moore et al., 2007)). At the start of each co-culture experiment, *Alteromonas* cells from stationary-stage cultures (24-72 hour old) were centrifuged (15 minutes, room temperature, 15,000g), the growth media decanted, and the cells re-suspended in Pro99. The *Prochlorococcus* cultures (growing exponentially) and the re-suspended *Alteromonas* cells were then counted using BD FACSCanto™ II Flow Cytometry Analyzer Systems (BD Biosciences). For each co-culture, $1x10^6$ *Prochlorococcus* cells mixed with $1x10^7$ *Alteromonas* cells. For mono-cultures, $1x10^6$ and $1x10^7$ were added for *Prochlorococcus* and *Alteromonas*, respectively. The experiment was performed using triplicate 20ml cultures in borosilicate test tubes (2.5cm diameter, 15cm length).

Fluorescence and Flow cytometry

Bulk chlorophyll fluorescence (FL) (ex440; em680) was measured almost daily using a Fluorescence Spectrophotometer (Cary Eclipse, Varian). Samples for flow cytometry were taken for cell numbers after 60, 100 and 140 days of experiment 1 (Figure 1 – figure supplement 1). Samples were fixed with glutaraldehyde (0.125% final concentration), incubated in the dark for 10 min and stored in -80 °C until analysis. Then, samples were thawed at room temperature and run on a BD FACSCanto™ II Flow Cytometry Analyzer Systems (BD Biosciences). To each sample, 2 µm diameter fluorescent beads (Polysciences, Warminster, PA, USA) were added as an internal standard. At first, the natural fluorescence of the cells (chlorophyll pigments) was examined to identify *Prochlorococcus*, identified based on the PerCP-A and FSC-H. Samples were then stained with SYBR Green I (Molecular Probes/ ThermoFisher) to a final concentration according to the manufacturer's instructions and the *Alteromonas* was counted. Data were acquired and processed with FlowJo software. Flow rates were determined several times during each running session, and the average value for a specific run was used for calculating cells per ml.

PCA ordination

PCA ordination was run on the growth curves. The Cumulative sum of Fluorescence measurements were standardized via standard scalar by subtracting the mean and scaling to unit variance of each feature. Ordination was computed via principal component analysis (PCA). Data preprocessing was done by pandas (0.25.0). Scaling and PCA was done using sklearn (0.21.2).

Growth rate

Growth was computed - by solving the equation:

$$N_t = N_0 \, e^{\mu(t-L)}$$

Where N_t represents the number of cells at time *t*, N_0 is the initial number of cells, μ is the growth rate, and *L* is the growth lag. The LAN transformed equation was used to compute growth rate:

$$\ln(N_t) = \ln(N_0) + \mu(t - L)$$

Linear regression was run on the growth phase, predicting $\ln(N_t)$ based on time *t* with $R^2 > 0.9$. The growth rate μ is the regression coefficient.

Fit to Decline models

The following functions were used to fit against the measured fluorescence:

Exponential: $FL_t = FL_{max} \, e^{-a(t-t_{max})}$

Bi-exponential: $FL_t = FL_{\max}(f \, e^{-a_1(t-t_{max})} + (1-f) \, e^{-a_2 \, (t-t_{max})})$

Harmonic: $FL_t = FL_{\max} \frac{1}{1+a\,t}$

Weibull: $FL_t = FL_{\max} \, e^{-a\,t^n}$

Where FL_t is the Fluorescence measured at time *t*, FL_{max} is the maximum fluorescence measured, t_{max} is the time when the fluorescence was highest, and *a, a1, a2, n, f* are the model parameters estimated by the fitting function.

The decline function was fit against each growth curve via curve_fit() function from scipy package (1.3.0), using the parameters: method='dogbox', loss='soft_l1', f_scale=0.1. Each model was fit using random initial parameter values and the initial values of 0.5 per parameter, and the fit with the lowest RSME selected. Goodness of fit was measures using root mean square error (RMSE).

In the Weibull model the time needed to reduce the population by *d* factors of 10 (t_{d2}) was estimated as in (Van Boekel, 2002), using the formula:

$$t_d = a \, (-ln(10^{-d})^{\frac{1}{n}})$$

500 **Random Forest Classification**

501 Random Forest Classification was run on the growth curves. To detect difference in the curve
502 pattern and not timing specific differences, the curves were aligned such that max growth point
503 are at time zero, and time points from 10 days prior to max growth to 80 days after were selected.
504 Since the specific measurement time points were different in different experiments and samples,
505 rolling average was used to get mean fluorescence per day, and interpolation used to fill in missing
506 measurements. The Fluorescence measurements were standardized via standard scalar by
507 subtracting the mean and scaling to unit variance of each feature. Random Forest model was run
508 in 10x cross validation to classify the curves by *Prochlorococcus* and by *Alteromonas* strains. To
509 find the most significant days in *Prochlorococcus* classification, the model was built 30 times and
510 the mean importance of all features (i.e., measurement days) calculated. Data preprocessing was
511 done by pandas (0.25.0). Scaling and model fitting using sklearn (0.21.2).

512 **Statistics**

513 Statistics were computed using the statsmodels package in python. Multi test correction was done
514 by t_test_pairwise() using Bonferroni correction. Permanova analysis by adonis2 from R vegan
515 package (R 3.61, vegan 2.5-7).

516 **DNA extraction, genome resequencing and SNP analysis**

517 Samples for genomic DNA sequencing was collected from parental strains, before experiment 1
518 and after 435 days from co-cultures (Figure 1- figure supplement 1, Figure 5a). Samples collected
519 on a 0.22 µm filter (Supor, Pall Corporation), filled with 1 ml of storage buffer (40 mM EDTA, 50
520 mM Tris pH=8.3, 0.75 M Soucrose) and stored at −80°C. Before extraction samples were thawed
521 on ice and storage buffer removed carefully. DNA extracted using DNeasy PowerWater Kit
522 (Qiagen) according to the kit's protocol. DNA samples (minimum concentration of 1ng/uL) were
523 submitted to the MIT BioMicroCenter in 96 well plate format. Samples were prepared for
524 sequencing using Nextera flex preparation for intact DNA (high throughput) and a size selection
525 of 300-600bp. DNA was sequenced using MiSeq flowcell (v3, 600nt). The samples have been
526 processed using the BMC/BCC 1.7 pipeline updated on 01/11/2019. The NexteraPE adapter and
527 the first 20 bases were trimmed by trimmomatic 0.39-1. And quality checked using fastqc and
528 multiqc. All samples were mapped to the reference genome and variant called using snippy (based
529 on bwa mem mapping, freebayes variant call, snpEff annotation). *Alteromonas* reads were
530 removed from Co-culture samples by first mapping to *Alteromonas* HOT1A3 (NCBI accession:
531 NZ_CP012202.1, NZ_CP012203.1), then running snippy a second time on reads that were not
532 mapped to Alteromonas, mapping against *Prochlorococcus* MIT9313 (NCBI accession:
533 NC_005071.1). The number of reads per sample was 550K-610K, 98-99% of the reads were
534 mapped successfully to MIT9313 genome yielding mean coverage of 29-42X, 99-100% of the
535 genes had >10X coverage. Mapping quality was assessed using qualimap. SNPs were called only if
536 the read depth was at lease 10 and the Genotype Quality, the Phred-scaled marginal (or
537 unconditional) probability of the called genotype was at least 20.

538

539

Acknowledgements

Daniel Segrè and Melisa Osborne for help with sequencing, Sher lab members and especially Natalie Andrawes for help in fluorescence measurements. Hans-Peter Grossart, Zhen Wu and Tal Luzzatto Knaan for critical reading of the manuscript. This work was supported by the Human Frontiers Science Program (grant RGP0020/2016, to DS) and the NSF-BSF program in Oceanography (grant 1635070/2016532, to DS).

References

Aharonovich, D., & Sher, D. (2016). Transcriptional response of Prochlorococcus to co-culture with a marine Alteromonas: Differences between strains and the involvement of putative infochemicals. *ISME Journal*, *10*(12), 2892–2906. https://doi.org/10.1038/ismej.2016.70

Amin, S. A., Hmelo, L. R., Van Tol, H. M., Durham, B. P., Carlson, L. T., Heal, K. R., Morales, R. L., Berthiaume, C. T., Parker, M. S., Djunaedi, B., Ingalls, A. E., Parsek, M. R., Moran, M. A., & Armbrust, E. V. (2015). Interaction and signalling between a cosmopolitan phytoplankton and associated bacteria. *Nature*, *522*(7554), 98–101. https://doi.org/10.1038/nature14488

Antoniewicz, M. R. (2020). A guide to deciphering microbial interactions and metabolic fluxes in microbiome communities. *Current Opinion in Biotechnology*, *64*, 230–237. https://doi.org/10.1016/j.copbio.2020.07.001

Bagchi, S. N., & Kleiner, D. (1990). Dismutation of hydroxylamine to ammonia and nitrite by a novel, membrane-bound enzyme from the cyanobacterium Phormidium uncinatum. *Biochimica et Biophysica Acta (BBA)/Protein Structure and Molecular*, *1041*(1), 9–13. https://doi.org/10.1016/0167-4838(90)90115-V

Bagchi, S. N., & Kleiner, D. (1991). Interrelationship between hydrogen peroxide, ammonia, glutamine, hydroxylamine and nitrite metabolism in the cyanobacterium Phormidium uncinatum. *Archives of Microbiology*, *156*(5), 367–369. https://doi.org/10.1007/BF00248712

Becker, J. W., Hogle, S. L., Rosendo, K., & Chisholm, S. W. (2019). Co-culture and biogeography of Prochlorococcus and SAR11. *ISME Journal*, *13*(6), 1506–1519. https://doi.org/10.1038/s41396-019-0365-4

Beckett, S. J., Demory, D., Coenen, A. R., Casey, J. R., Dugenne, M., Follett, C. L., Connell, P., Carlson, M. C. G., Hu, S. K., Wilson, S. T., Becker, K. W., Mende, D. R., Armbrust, E. V., White, A. E., Ribalet, F., & Weitz, J. S. (2021). *Diel population dynamics and mortality of Prochlorococcus in the North Pacific Subtropical Gyre*. 1–20.

Biller, S. J., Berube, P. M., Lindell, D., & Chisholm, S. W. (2015). Prochlorococcus: The structure and function of collective diversity. *Nature Reviews Microbiology*, *13*(1), 13–27. https://doi.org/10.1038/nrmicro3378

Biller, S. J., Coe, A., & Chisholm, S. W. (2016). Torn apart and reunited: Impact of a heterotroph on the transcriptome of Prochlorococcus. *ISME Journal*, *10*(12), 2831–2843. https://doi.org/10.1038/ismej.2016.82

Brouwer, A. F., Eisenberg, M. C., Remais, J. V., Collender, P. A., Meza, R., & Eisenberg, J. N. S. (2017). Modeling Biphasic Environmental Decay of Pathogens and Implications for Risk Analysis. *Environmental Science and Technology*, *51*(4), 2186–2196. https://doi.org/10.1021/acs.est.6b04030

Christie-Oleza, J. A., Sousoni, D., Lloyd, M., Armengaud, J., & Scanlan, D. J. (2017). Nutrient recycling facilitates long-term stability of marine microbial phototroph-heterotroph interactions. *Nature Microbiology*, *2*(June). https://doi.org/10.1038/nmicrobiol.2017.100

Cirri, E., & Pohnert, G. (2019). Algae−bacteria interactions that balance the planktonic microbiome. *New Phytologist*, *223*(1), 100–106. https://doi.org/10.1111/nph.15765

Coe, A., Biller, S. J., Thomas, E., Boulias, K., Bliem, C., Dooley, K., Rasmussen, A. N., Legault, K., Keefe, T. J. O., Eric, L., & Chisholm, S. W. (2020). *Coping with darkness: The adaptive response of marine picocyanobacteria to repeated light energy deprivation*. 1–32.

Coe, A., Ghizzoni, J., LeGault, K., Biller, S., Roggensack, S. E., & Chisholm, S. W. (2016). Survival of Prochlorococcus in extended darkness. *Limnology and Oceanography*, *61*(4), 1375–1388. https://doi.org/10.1002/lno.10302

Cole, J. J. (1982). *INTERACTIONS BETWEEN*. 291–314.

Cordero, O. X., Wildschutte, H., Kirkup, B., Proehl, S., Ngo, L., Hussain, F., Le Roux, F., Mincer, T., Polz, M. F., & Roux, F. Le. (2012). Ecological Populations of BacteriaAct as Socially Cohesive Units ofAntibiotic Production and Resistance. *Science (New York, N.Y.)*, *337*(September), 1228–1231. https://doi.org/10.1126/science.1219385

Crane, S. R., & Moore, J. A. (1986). Modeling enteric bacterial die-off: A review. *Water, Air, & Soil Pollution*, *27*(3–4), 411–439. https://doi.org/10.1007/BF00649422

Cubillos-Ruiz, A., Berta-Thompson, J. W., Becker, J. W., Van Der Donk, W. A., & Chisholm, S. W. (2017). Evolutionary radiation of lanthipeptides in marine cyanobacteria. *Proceedings of the National Academy of Sciences of the United States of America*, *114*(27), E5424–E5433. https://doi.org/10.1073/pnas.1700990114

Diner, R. E., Schwenck, S. M., McCrow, J. P., Zheng, H., & Allen, A. E. (2016). Genetic manipulation of competition for nitrate between heterotrophic bacteria and diatoms. *Frontiers in Microbiology*, *7*(JUN). https://doi.org/10.3389/fmicb.2016.00880

Dutkiewicz, S., Follows, M., Marshall, J., & Gregg, W. W. (2001). Interannual variability of phytoplankton abundances in the North Atlantic. *Deep Sea Research Part II: Topical Studies in Oceanography*, *48*(10), 2323–2344.

Field, C. B., Behrenfeld, M. J., Randerson, J. T., & Falkowski, P. (1998). Primary production of the biosphere: Integrating terrestrial and oceanic components. *Science*, *281*(5374), 237–240. https://doi.org/10.1126/science.281.5374.237

Finkel, S. E., & Kolter, R. (1999). Evolution of microbial diversity during prolonged starvation. *Proceedings of the National Academy of Sciences of the United States of America*, *96*(7), 4023–4027. https://doi.org/10.1073/pnas.96.7.4023

Foster, K. R., & Bell, T. (2012). Competition, not cooperation, dominates interactions among culturable microbial species. *Current Biology*, *22*(19), 1845–1850.

https://doi.org/10.1016/j.cub.2012.08.005

Fritts, R. K., McCully, A. L., & McKinlay, J. B. (2021). Extracellular Metabolism Sets the Table for Microbial Cross-Feeding. *Microbiology and Molecular Biology Reviews*, *85*(1). https://doi.org/10.1128/mmbr.00135-20

Gau, A. E., Heindl, A., Nodop, A., Kahmann, U., & Pistorius, E. K. (2007). L-amino acid oxidases with specificity for basic L-amino acids in cyanobacteria. *Zeitschrift Fur Naturforschung - Section C Journal of Biosciences*, *62*(3–4), 273–284. https://doi.org/10.1515/znc-2007-3-419

Gralka, M., Szabo, R., Stocker, R., & Cordero, O. X. (2020). Trophic Interactions and the Drivers of Microbial Community Assembly. *Current Biology*, *30*(19), R1176–R1188. https://doi.org/10.1016/j.cub.2020.08.007

Grossart, H. P. (1999). Interactions between marine bacteria and axenic diatoms (Cylindrotheca fusiformis, Nitzschia laevis, and Thalassiosira weissflogii) incubated under various conditions in the lab. *Aquatic Microbial Ecology*, *19*(1), 1–11. https://doi.org/10.3354/ame019001

Grossart, H. P., & Simon, M. (2007). Interactions of planktonic algae and bacteria: Effects on algal growth and organic matter dynamics. *Aquatic Microbial Ecology*, *47*(2), 163–176. https://doi.org/10.3354/ame047163

Grossowicz, M., Roth-Rosenberg, D., Aharonovich, D., Silverman, J., Follows, M. J., & Sher, D. (2017). Prochlorococcus in the lab and in silico: The importance of representing exudation. *Limnology and Oceanography*, *62*(2), 818–835. https://doi.org/10.1002/lno.10463

Hackl, T., Laurenceau, R., Ankenbrand, M. J., Bliem, C., Cariani, Z., Thomas, E., Dooley, K. D., Arellano, A. A., Hogle, S. L., Berube, P., Leventhal, G. E., Luo, E., Eppley, J., Zayed, A. A., Beaulaurier, J., Stepanauskas, R., Sullivan, M. B., DeLong, E. F., Biller, S. J., & Chisholm, S. W. (2021). Novel Integrative Elements and Genomic Plasticity in Ocean Ecosystems. *SSRN Electronic Journal*. https://doi.org/10.2139/ssrn.3817805

Harrington, V., Lau, L., Seddu, K., & Suez, J. (2021). *Ecology and Medicine Converge at the Microbiome-Host*. *6*(4), 4–8.

Hennon, G. M., Morris, J. J., Haley, S. T., Zinser, E. R., Durrant, A. R., Entwistle, E., Dokland, T., & Dyhrman, S. T. (2018). The impact of elevated CO 2 on Prochlorococcus and microbial interactions with â € helper' bacterium Alteromonas. *ISME Journal*, *12*(2), 520–531. https://doi.org/10.1038/ismej.2017.189

Hogg, T., Mechold, U., Malke, H., Cashel, M., & Hilgenfeld, R. (2004). Conformational antagonism between opposing active sites in a bifunctional RelA/SpoT homolog modulates (p)ppGpp metabolism during the stringent response. *Cell*, *117*(1), 57–68. https://doi.org/10.1016/S0092-8674(04)00260-0

Hou, S., López-Pérez, M., Pfreundt, U., Belkin, N., Stüber, K., Huettel, B., Reinhardt, R., Berman-Frank, I., Rodriguez-Valera, F., & Hess, W. R. (2018). Benefit from decline: The primary transcriptome of Alteromonas macleodii str. Te101 during Trichodesmium demise. *ISME Journal*, *12*(4), 981–996. https://doi.org/10.1038/s41396-017-0034-4

Kettler, G. C., Martiny, A. C., Huang, K., Zucker, J., Coleman, M. L., Rodrigue, S., Chen, F., Lapidus,

A., Ferriera, S., Johnson, J., Steglich, C., Church, G. M., Richardson, P., & Chisholm, S. W. (2007). Patterns and implications of gene gain and loss in the evolution of Prochlorococcus. *PLoS Genetics*, *3*(12), 2515–2528. https://doi.org/10.1371/journal.pgen.0030231

Klähn, S., Steglich, C., Hess, W. R., & Hagemann, M. (2010). Glucosylglycerate: A secondary compatible solute common to marine cyanobacteria from nitrogen-poor environments. *Environmental Microbiology*, *12*(1), 83–94. https://doi.org/10.1111/j.1462-2920.2009.02045.x

Koch, H., Dürwald, A., Schweder, T., Noriega-Ortega, B., Vidal-Melgosa, S., Hehemann, J. H., Dittmar, T., Freese, H. M., Becher, D., Simon, M., & Wietz, M. (2019). Biphasic cellular adaptations and ecological implications of Alteromonas macleodii degrading a mixture of algal polysaccharides. *ISME Journal*, *13*(1), 92–103. https://doi.org/10.1038/s41396-018-0252-4

Koch, H., Germscheid, N., Freese, H. M., Noriega-Ortega, B., Lücking, D., Berger, M., Qiu, G., Marzinelli, E. M., Campbell, A. H., Steinberg, P. D., Overmann, J., Dittmar, T., Simon, M., & Wietz, M. (2020). Genomic, metabolic and phenotypic variability shapes ecological differentiation and intraspecies interactions of Alteromonas macleodii. *Scientific Reports*, *10*(1), 1–14. https://doi.org/10.1038/s41598-020-57526-5

Latifi, A., Ruiz, M., & Zhang, C. C. (2009). Oxidative stress in cyanobacteria. *FEMS Microbiology Reviews*, *33*(2), 258–278. https://doi.org/10.1111/j.1574-6976.2008.00134.x

Li, B., Sher, D., Kelly, L., Shi, Y., Huang, K., Knerr, P. J., Joewono, I., Rusch, D., Chisholm, S. W., & Van Der Donk, W. A. (2010). Catalytic promiscuity in the biosynthesis of cyclic peptide secondary metabolites in planktonic marine cyanobacteria. *Proceedings of the National Academy of Sciences of the United States of America*, *107*(23), 10430–10435. https://doi.org/10.1073/pnas.0913677107

Long, R. A., & Azam, F. (2001). Microscale patchiness of bacterioplankton assemblage richness in seawater. *Aquatic Microbial Ecology*, *26*(2), 103–113. https://doi.org/10.3354/ame026103

López-Pérez, M., & Rodriguez-Valera, F. (2016). Pangenome evolution in themarine bacterium alteromonas. *Genome Biology and Evolution*, *8*(5), 1556–1570. https://doi.org/10.1093/gbe/evw098

Malmstrom, R. R., Coe, A., Kettler, G. C., Martiny, A. C., Frias-Lopez, J., Zinser, E. R., & Chisholm, S. W. (2010). Temporal dynamics of Prochlorococcus ecotypes in the Atlantic and pacific oceans. *ISME Journal*, *4*(10), 1252–1264. https://doi.org/10.1038/ismej.2010.60

Mcdonagh, B., Domínguez-Martín, M. A., Gómez-Baena, G., López-Lozano, A., Diez, J., Bárcena, J. A., & García Fernández, J. M. (2012). Nitrogen starvation induces extensive changes in the redox proteome of Prochlorococcus sp. strain SS120. *Environmental Microbiology Reports*, *4*(2), 257–267. https://doi.org/10.1111/j.1758-2229.2012.00329.x

Monod, J. (1949). a Certain Number. *Annual Reviews in M*, *3*(XI), 371–394.

Moore, L. R., Coe, A., Zinser, E. R., Saito, M. A., Sullivan, M. B., Lindell, D., Frois-Moniz, K., Waterbury, J., & Chisholm, S. W. (2007). Culturing the marine cyanobacterium Prochlorococcus. *Limnology and Oceanography: Methods*, *5*(OCT), 353–362. https://doi.org/10.4319/lom.2007.5.353

Moore, S. K., Baird, M. E., & Suthers, I. M. (2006). Relative effects of physical and biological processes on nutrient and phytoplankton dynamics in a shallow estuary after a storm event. *Estuaries and Coasts*, *29*(1), 81–95. https://doi.org/10.1007/BF02784701

Morris, J. J., Johnson, Z. I., Szul, M. J., Keller, M., & Zinser, E. R. (2011). Dependence of the cyanobacterium Prochlorococcus on hydrogen peroxide scavenging microbes for growth at the ocean's surface. *PLoS ONE*, *6*(2). https://doi.org/10.1371/journal.pone.0016805

Morris, J. Jeffrey, Kirkegaard, R., Szul, M. J., Johnson, Z. I., & Zinser, E. R. (2008). Facilitation of robust growth of Prochlorococcus colonies and dilute liquid cultures by "helper" heterotrophic bacteria. *Applied and Environmental Microbiology*, *74*(14), 4530–4534. https://doi.org/10.1128/AEM.02479-07

Morris, J. Jeffrey, Lenski, R. E., & Zinser, E. R. (2012). The black queen hypothesis: Evolution of dependencies through adaptive gene loss. *MBio*, *3*(2), 1–7. https://doi.org/10.1128/mBio.00036-12

Murray A.G. and Parslow J.S. (1999). The analysis of alternative formulations in a simple model of a coastal ecosystem. *Ecological Modelling*, *119*(2–3), 149–166.

Pacheco, A. R., Osborne, M. L., & Segrè, D. (2021). Non-additive microbial community responses to environmental complexity. *Nature Communications*, *12*(1), 1–11. https://doi.org/10.1038/s41467-021-22426-3

Patra, P., & Klumpp, S. (2013). Population Dynamics of Bacterial Persistence. *PLoS ONE*, *8*(5). https://doi.org/10.1371/journal.pone.0062814

Pedler, B. E., Aluwihare, L. I., & Azam, F. (2014). Single bacterial strain capable of significant contribution to carbon cycling in the surface ocean. *Proceedings of the National Academy of Sciences of the United States of America*, *111*(20), 7202–7207. https://doi.org/10.1073/pnas.1401887111

Pruitt, K. M., & Kamau, D. N. (1993). Mathematical models of bacterial growth, inhibition and death under combined stress conditions. *Journal of Industrial Microbiology*, *12*(3–5), 221–231. https://doi.org/10.1007/BF01584194

Ramanan, R., Kim, B. H., Cho, D. H., Oh, H. M., & Kim, H. S. (2016). Algae-bacteria interactions: Evolution, ecology and emerging applications. *Biotechnology Advances*, *34*(1), 14–29. https://doi.org/10.1016/j.biotechadv.2015.12.003

Ratzke, C., & Gore, J. (2017). Modifying and reacting to the environmental pH drives bacterial interactions. *Modifying and Reacting to the Environmental PH Can Drive Bacterial Interactions*, 136838. https://doi.org/10.1101/136838

Rocap, G., Larimer, F. W., Lamerdin, J., Malfatti, S., Chain, P., Ahlgren, N. A., Arellano, A., Coleman, M., Hauser, L., Hess, W. R., Johnson, Z. I., Land, M., Lindell, D., Post, A. F., Regala, W., Shah, M., Shaw, S. L., Steglich, C., Sullivan, M. B., … Chisholm, S. W. (2003). Genome divergence in two Prochlorococcus ecotypes reflects oceanic niche differentiation. *Nature*, *424*(6952), 1042–1047. https://doi.org/10.1038/nature01947

Roth-Rosenberg, D., Aharonovich, D., Luzzatto-Knaan, T., Vogts, A., Zoccarato, L., Eigemann, F., Nago, N., Grossart, H. P., Voss, M., & Sher, D. (2020). Prochlorococcus cells rely on microbial interactions rather than on chlorotic resting stages to survive long-term nutrient

starvation. *MBio*, *11*(4), 1–13. https://doi.org/10.1128/mBio.01846-20

Saito, M. A., McIlvin, M. R., Moran, D. M., Goepfert, T. J., DiTullio, G. R., Post, A. F., & Lamborg, C. H. (2014). Multiple nutrient stresses at intersecting Pacific Ocean biomes detected by protein biomarkers. *Science*, *345*(6201), 1173–1177. https://doi.org/10.1126/science.1256450

Schriek, S., Rückert, C., Staiger, D., Pistorius, E. K., & Michel, K. P. (2007). Bioinformatic evaluation of L-arginine catabolic pathways in 24 cyanobacteria and transcriptional analysis of genes encoding enzymes of L-arginine catabolism in the cyanobacterium Synechocystis sp. PCC 6803. *BMC Genomics*, *8*, 1–28. https://doi.org/10.1186/1471-2164-8-437

Segev, E., Wyche, T. P., Kim, K. H., Petersen, J., Ellebrandt, C., Vlamakis, H., Barteneva, N., Paulson, J. N., Chai, L., Clardy, J., & Kolter, R. (2016). Dynamic metabolic exchange governs a marine algal-bacterial interaction. *ELife*, *5*(NOVEMBER2016), 1–28. https://doi.org/10.7554/eLife.17473

Seyedsayamdost, M. R., Case, R. J., Kolter, R., & Clardy, J. (2011). The Jekyll-and-Hyde chemistry of phaeobacter gallaeciensis. *Nature Chemistry*, *3*(4), 331–335. https://doi.org/10.1038/nchem.1002

Seymour, J. R., Amin, S. A., Raina, J. B., & Stocker, R. (2017). Zooming in on the phycosphere: The ecological interface for phytoplankton-bacteria relationships. *Nature Microbiology*, *2*(May). https://doi.org/10.1038/nmicrobiol.2017.65

Sher, D., Thompson, J. W., Kashtan, N., Croal, L., & Chisholm, S. W. (2011). Response of Prochlorococcus ecotypes to co-culture with diverse marine bacteria. *ISME Journal*, *5*(7), 1125–1132. https://doi.org/10.1038/ismej.2011.1

Shoemaker, W. R., Jones, S. E., Muscarella, M. E., Behringer, M. G., Lehmkuhl, B. K., & Lennon, J. T. (2021). Microbial population dynamics and evolutionary outcomes under extreme energy limitation. *Proceedings of the National Academy of Sciences of the United States of America*, *118*(33), 1–8. https://doi.org/10.1073/pnas.2101691118

Steinchen, W., & Bange, G. (2016). The magic dance of the alarmones (p)ppGpp. *Molecular Microbiology*, *101*(4), 531–544. https://doi.org/10.1111/mmi.13412

Teeling, H., Fuchs, B. M., Becher, D., Klockow, C., Gardebrecht, A., Bennke, C. M., Kassabgy, M., Huang, S., Mann, A. J., Waldmann, J., Weber, M., Klindworth, A., Otto, A., Lange, J., Bernhardt, J., Reinsch, C., Hecker, M., Peplies, J., Bockelmann, F. D., … Amann, R. (2012). Substrate-controlled succession of marine bacterioplankton populations induced by a phytoplankton bloom. *Science*, *336*(6081), 608–611. https://doi.org/10.1126/science.1218344

Ting, C. S., Hsieh, C., Sundararaman, S., Mannella, C., & Marko, M. (2007). Cryo-electron tomography reveals the comparative three-dimensional architecture of Prochlorococcus, a globally important marine cyanobacterium. *Journal of Bacteriology*, *189*(12), 4485–4493. https://doi.org/10.1128/JB.01948-06

Tolonen, A. C., Aach, J., Lindell, D., Johnson, Z. I., Rector, T., Steen, R., Church, G. M., & Chisholm, S. W. (2006). Global gene expression of Prochlorococcus ecotypes in response to changes in nitrogen availability. *Molecular Systems Biology*, *2*.

https://doi.org/10.1038/msb4100087

Ustick, L. J., Larkin, A. A., Garcia, C. A., Garcia, N. S., Brock, M. L., Lee, J. A., Wiseman, N. A., Keith Moore, J., & Martiny, A. C. (2021). Metagenomic analysis reveals global-scale patterns of ocean nutrient limitation. *Science*, *372*(6539), 287–291. https://doi.org/10.1126/science.abe6301

Van Boekel, M. A. J. S. (2002). On the use of the Weibull model to describe thermal inactivation of microbial vegetative cells. *International Journal of Food Microbiology*, *74*(1–2), 139–159. https://doi.org/10.1016/S0168-1605(01)00742-5

Vetsigian, K., Jajoo, R., & Kishony, R. (2011). Structure and evolution of streptomyces interaction networks in soil and in silico. *PLoS Biology*, *9*(10). https://doi.org/10.1371/journal.pbio.1001184

Warringer, J., Anevski, D., Liu, B., & Blomberg, A. (2008). Chemogenetic fingerprinting by analysis of cellular growth dynamics. *BMC Chemical Biology*, *8*, 1–10. https://doi.org/10.1186/1472-6769-8-3

Weisskopf, L., Schulz, S., & Garbeva, P. (2021). Microbial volatile organic compounds in intra-kingdom and inter-kingdom interactions. *Nature Reviews Microbiology*, *19*(6), 391–404. https://doi.org/10.1038/s41579-020-00508-1

Yelton, A. P., Acinas, S. G., Sunagawa, S., Bork, P., Pedrós-Alió, C., & Chisholm, S. W. (2016). Global genetic capacity for mixotrophy in marine picocyanobacteria. *ISME Journal*, *10*(12), 2946–2957. https://doi.org/10.1038/ismej.2016.64

Zheng, Q., Wang, Y., Lu, J., Lin, W., Chen, F., & Jiao, N. (2020). Metagenomic and metaproteomic insights into photoautotrophic and heterotrophic interactions in a Synechococcus culture. *MBio*, *11*(1). https://doi.org/10.1128/mBio.03261-19

Zoccarato, L., Sher, D., Miki, T., Segrè, D., & Grossart, H. P. (2020). Comparative whole-genome approach to identify traits underlying microbial interactions. *BioRxiv*, 1–53. https://doi.org/10.1101/2020.06.30.179929